

# **Exploring Molecules, Materials and Bio-Materials for Sustainable Society**

**Editors: Dr. Gobinda Prasad Sahoo  
Dr. Koushik Chandra**

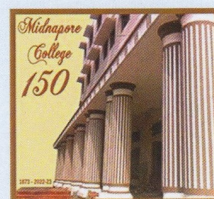
**08<sup>th</sup> to 10<sup>th</sup> September, 2022**

**International Symposium Proceeding**



**MIDNAPORE COLLEGE (AUTONOMOUS)**

**Fine Art**  
DIGITAL & BOOK PRINT







## Proceedings

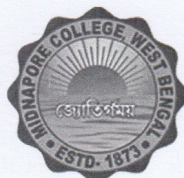
# Exploring Molecules, Materials and Bio-Materials for Sustainable Society

### *Editors*

**Dr. Gobinda Prasad Sahoo**  
Department of Chemistry  
Midnapore College (Autonomous)

**Dr. Koushik Chandra**  
Department of Chemistry  
Midnapore College (Autonomous)

*Published by*



Midnapore College (Autonomous)  
Midnapore, West Bengal-721101, India

*Sponsored by*  
SERB, New Delhi







## Contents

Sr. No.	Title and Authors	Page no.
1	<b>Screening of Biologically active Ferrocene based compounds as potential inhibitors of RNA dependent RNA polymerase (RdRp) of SARS-CoV-2: A molecular docking, DFT calculations and ADME study</b> <i>Avishek Ghosh*, Putul Karan, Bhagabati Bera, Dr. Maidul Hossain and Dr. Harekrushna Sahoo</i>	1
2	<b>Cycloaddition of Azomethine Imines and Azomethine Ylides for Synthesizing Five Membered Heterocycles</b> <i>Abdul Motaleb</i>	9
3	<b>Synthesis of Cadmium (II) complex with tridentate O,N,O-donor Schiff base and biological application</b> <i>Animesh Patra</i>	15
4	<b>NMR analysis of a heteropolysaccharide isolated from hot water extract of pods (fruits) of <i>Moringa oleifera</i> (Sajina)</b> <i>Sadhan Kumar Roy</i>	19
5	<b>Recent Synthetic Approaches of Organoselenium and Selenophosphorus Compounds</b> <i>Samir Kumar Bhunia,* and Manas Kumar Manna</i>	24
6	<b>Development of pH-Sensitive Colorimetric Polymer Film using Chitosan and Congo Red</b> <i>Uttam Samanta, Souptik Ghos and Subhankar Singha*</i>	31
7	<b>Green Synthesis of Silver nanoparticles from <i>Ocimum sanctum</i> (Tulsi) leaf Extract: An eco-friendly and biogenic approach</b> <i>Amar Ghosh, Animesh Halder, Arpita Nandy, Sanat Karmakar, Dulal Senapati,* and Ujjal Kumar Sur</i>	37
8	<b>Computational Spectroscopy of diamondoids: Tuning the optical gaps</b> <i>Shiladitya Banerjee</i>	43
9	<b>IBX and Modified-IBXs as Catalyst in Organic Synthesis</b> <i>Kalyan senapati</i>	47
10	<b>Study of Fluorescence and Computational Analysis on Advanced Glycation of Bovine Serum Albumin with Glucose</b> <i>Charu Chand Hansda, Santu Bhunia, Arindam Bankura and Koushik Chandra*</i>	51
11	<b>Metal Nanoparticles: Green synthesis and their application</b> <i>Chhabi Garai</i>	56
12	<b>Acid catalyzed synthesis of steroidal triazolo-pyrimidine derivatives under microwave irradiation</b> <i>Abad Ali</i>	61
13	<b>Ferrocene: Structure and its reactivity reactivity</b> <i>Avishek Ghosh</i>	67
14	<b>Epidemiology, Pathophysiology and Molecular Pathogenesis of Hodgkin's Lymphoma</b> <i>Madhurima Maity and Subho Ghosh*</i>	70
15	<b>A simple design of a fluorescent chemosensor for preferential recognition of Al (III) ion</b> <i>Ansuman Bej and Tarun Mistri*</i>	75
16	<b>Antimicrobial Resistance- Beta Lactamase-A global Threat</b> <i>Riya Karan and Partha Pratim Jana*</i>	80
17	<b>Recognition of Reactive Sites of N-Linkage glycoprotein Monomer in Minimal Amino Acid Sequence: A DFT Based Study</b> <i>Hasibul Beg</i>	84
18	<b>Synthesis of Carbon Nano Dots from shankhalu (<i>Pachyrhizus erosus</i>)</b> <i>Madhumita Hazra</i>	89
19	<b>The DNA intercalative trinuclear Cu(II) complex</b> <i>Malay Dolai* and Urmila Saha</i>	92





## Screening of Biologically active Ferrocene based compounds as potential inhibitors of RNA dependent RNA polymerase (RdRp) of SARS-CoV-2: A molecular docking, DFT calculations and ADME study

<sup>1</sup>Avishek Ghosh\*, <sup>1</sup>Putul Karan, <sup>1</sup>Bhagabati Bera, <sup>2</sup>Dr. Maidul Hossain, <sup>3</sup>Dr. Harekrushna Sahoo

<sup>1</sup>Department of Chemistry, Midnapore City College, Kuturia, Bhadutala, Paschim Medinipur, West Bengal 721129, India.

<sup>2</sup>Department of Chemistry and Chemical technology, Vidyasagar University, West Bengal. Medinipur 721102

<sup>3</sup>Department of Chemistry, National Institute of Technology Rourkela, Rourkela, Odisha, India

\*Corresponding Author E-mail: [avishek.ghosh.mcc@gmail.com](mailto:avishek.ghosh.mcc@gmail.com), Contact number: +918280103667

### ABSTRACT

The in-silico molecular docking study has great potential to find out the active compound against various proteins of different types of pathogens. Keep in this mind we employed these techniques to find out ferrocene based bioactive compounds as potential inhibitors against RdRp of SARS-COV-2. DFT calculation of 45 ferrocenyl systems have been carried out. Among the 45 reported ferrocene-based antiviral, antibacterial, antiparasitic, antifungal compounds; 19 have been found as a better potential inhibitor of RdRp of SARS-COV-2 in comparison with remdesivir. The antiviral (hepatitis C virus) agent, i.e., 1,1'-diarylated ferrocene derivative (1) shows highest binding affinity (-9.6 kcal/mol) with RdRp protein of SARS-COV-2. The compound (7), Ferrocenyle-6-aminopenicillanic acid bioconjugate active against staphylococcus aureus and staphylococcus epidermidis and compound (6) anti-parasitic Ferrocene based Mefloquine derivative effective against entamoeba histolytica and plasmodium falciparum has shown a promising result in the inhibition of the function of RdRp. The ADME study shows 3d and 3e compounds have promising binding affinity as well as physiochemical and pharmacokinetic properties. We believe that this finding will be helpful to design ferrocene based potential drug for fight against SARS-CoV-2.

**Keywords:** Coronavirus COVID-19, Molecular docking, Ferrocenyl derivatives.

### Introduction

In 2019, a contagious respiratory disease has been spread from China to all over the world named as the SARS-CoV-2 (Wang & Guan 2020). On Jan 30, 2020, World Health Organization (WHO) declared an emergency alert to the human civilization and on Mar 11, 2020 declared this disease as a global pandemic (Wang & Guan 2020; Khaerunnisa et al. 2020). Scientific community different part of the globe was starting search and tries to understand the nature of the virus and find out the effective drugs against the virus to give better treatment for this disease (Shah et al. 2021). After a detailed research it has been established that human to human transmission via droplets is the main route for transmission of this virus to the susceptible population (Jayaweera et al. 2020) and mainly three viral proteins help the virus to spread, i.e., M<sup>pro</sup> (Main protease) (Jin et al. 2020), Spike protein (Shang et al. 2020) and RdRp (RNA dependent RNA Polymerase) (Gao et al. 2020). A key step to stop the progression of SARS-CoV-2 virus is to inhibit the replication process, which can be achieved by blocking the RdRp protein using suitable drug, as RdRp protein is vital component for replication (Yin et al. 2020). Computational approaches have played a crucial role to discover, develop and analyse drugs and biologically active molecules using natural or synthetic ingredients (Aouidate et al. 2018a; Aouidate et al. 2018b; Lipinski et al. 1997). In the present study, molecular docking (Channotiya et al. 2021) method is used to screen the appropriate biological active ferrocene derivatives molecule against SARS-COV-2.

In recent years of chemistry of ferrocene and its derivatives have attracted significant interest in medicinal chemistry which is an active research area (Kealy & Pauson 1951; Lal et al. 2011). The introduction of the lipophilic organometallic moiety ferrocene and its derivatives are associated with a wide range of biological activities for the development of more efficient drugs. Many research groups have designed and synthesized different type of bioactive ferrocene compounds (Ludwig et al. 2019) and can be used as Antiparasitic, Antimalarial (Peter & Aderibigbe 2019), anticancer (Biot et al. 2020; Asghar et al. 2018), antibacterial (Peter and Aderibigbe 2019) agents. Earlier studies show that combining ferrocene with known antimalarial, anti-cancer drugs can increase the effectiveness of the drugs (Chohan 2006). In this study first time, biologically active ferrocene-based compounds are virtually screened against the RdRp (6M71) of SARS-CoV-2 to understand the effectiveness of ferrocenyl compounds as an anti-viral drug against covid19 which may give some idea to create a new window to find out new class of drug for covid-19.





## Materials and Methods

To verify the best binding mode of ferrocene-based compounds with RdRp of SARS-CoV-2, blind docking procedures is performed using AutoDock vina software. The crystal structure of RdRp (6M71) has been downloaded from the Protein Data Bank (<http://www.rcsb.org/pdb/home/home.do>). The 3D molecular structures of 45 ferrocene based biological active molecules have been sketched using Avogadro software and then optimize using Orca 4.2.1 at the DFT/B3LYP/def2-SVP level. Using AutoDock tools, the water molecules, ions, and other ligands present in the protein targets RdRp (6M71) have been removed and the structures have been converted into PDBQT format for molecular docking analysis. The grid box is set centered on the RdRp molecule with dimensions of  $119.721 \times 123.605 \times 120.3 \text{ \AA}^3$  and a spacing of  $1.0 \text{ \AA}$ . After that, the docking study has been performed to seek the best binding site of ferrocene-based compounds in RdRp with the default parameters. For each docking procedure, 9 conformations are considered, of which, the conformation with lowest binding energy is selected and analysed using the Biovia Discovery Studio Visualizer version 2016 (Dassault systems Bioviacorp) (Dassault Systemes BIOVIA, 2016) and PyMOL 2.3 (Schrodinger LLC). The ADME study, in the present work is carried out using a free and acceptable online server, that is, swissADME (<http://www.swissadme.ch>) has been used to calculate various physiochemical and pharmacokinetic properties of the ferrocene-based compounds.

## Results and discussion

Molecular docking study of ferrocene base compounds

In this study, NSP12 chain of RdRp of SARS Co-V-2 is virtually screened with 45 different reported biological active ferrocene-based compounds. The 3D structures of ferrocenyl derivatives are drawn in Avogadro and optimise with Orca using DFT method in B3LYP level with def2-SVP basic set. The cut off value of docking score has been set  $> -8.0 \text{ Kcal/mol}$  because in our in-silico study the docking score of Remdesivir against RdRp (6M71) of SARS-CoV-2 is found  $-8.1 \text{ kcal/mol}$ . The best 19 ferrocene-based ligands have been chosen on the basis of their docking score and summarised in Table1.

Antiviral (hepatitis C virus) agent 1,1'-diarylated ferrocene derivative (1), reported by Venkat et al in 2018 shows highest binding affinity  $-9.6 \text{ kcal/mol}$  with RdRp of covid 19 (Gadhachanda et al. 2018; Ruiz et al. 2017). The 16 anti-parasitic pyrimidine based ferrocene derivative shows anti-viral activity against RdRp of Covid-19. Morpholine linked pyrimidine based ferrocenyl system (2a),(2b),(2c),(2d) and (2e) shows binding affinity  $-8.8 \text{ kcal/mol}$ ,  $-9.0 \text{ kcal/mol}$ ,  $-8.8 \text{ kcal/mol}$ ,  $-8.7 \text{ kcal/mol}$  and  $-8.0 \text{ kcal/mol}$  respectively. Piperidine linked pyrimidine based ferrocenyl system (3a),(3b) (3c), (3d) and (3e) shows binding affinity  $-9.2 \text{ kcal/mol}$ ,  $-8.7 \text{ kcal/mol}$ ,  $-8.4 \text{ kcal/mol}$ ,  $-8.4 \text{ kcal/mol}$  and  $-8.3 \text{ kcal/mol}$  respectively (Parveen et al. 2010). Pyrrolidine substituted pyrimidine based ferrocenyl compounds (4a), (4b), (4c) and (4d) shows binding affinity  $-8.4 \text{ kcal/mol}$ ,  $-8.2 \text{ kcal/mol}$ ,  $-8.1 \text{ kcal/mol}$  and  $-8.0 \text{ kcal/mol}$  correspondingly (Parveen et al. 2010). Ferrocene containing thiazepine derivative (5a) (García et al. 2017) and (5b) (Parveen et al. 2018) effectively binds with RdRp of covid 19 with the binding affinity  $-9.0 \text{ kcal/mol}$  and  $-8.6 \text{ kcal/mol}$ . The Ferrocene based Mefloquine derivative (6), active against plasmodium falciparum shows binding affinity against RdRp of Covid19 is  $-8.9 \text{ kcal/mol}$  (Biot et al. 2018; Herrmann et al. 2012). The anti-bacterial Ferrocenyle-6-aminopenicillanic acid bioconjugate (7), active against Staphylococcus aureus and Staphylococcus epidermidis shows binding affinity  $-8.2 \text{ kcal/mol}$  against RdRp of covid-19 (Skiba et al. 2012; Lewandowski et al. 2015).

The in-silico binding study shows that compound 1 forms two hydrogen bonding interactions with Asn497A and Lys621A, one pi-anion interaction with amino acid Asp623A. It also forms seven pi-alkyl interactions with Tyr455A, Lys500A, Arg553A, Val557A, Pro620A, Ala685A, twelve hydrophobic interactions with Asn496A, Ser501A, Lys545A, Lys551A, Arg555A, Ala558A, Gly559A, Arg569A, Asp618A, Tyr619A, Ser682A and Gly683A and an unfavourable donor-donor interaction with Cys622A amino acids (Fig.2A). (binding affinity  $-9.6 \text{ kcal/mol}$ ).

Next, compound 2a interacts with Val315A, Pro461A and Pro677A amino acids using pi-alkyl interactions, Arg349A amino acid by pi-cation interactions and Ser318A, Thr319A, Phe321A, Pro323A, Phe326A, Glu350A, Thr394A, Cys395A, Phe396A, Arg457A, Asn459A, Asn628A amino acids via hydrophobic interactions (Fig. 2B). (binding affinity  $-8.8 \text{ kcal/mol}$ )

Compound 2b also forms hydrogen bonding interaction with Phe396A, pi-alkyl interactions with Val315A, Pro323A, Cys395A, Pro461A, Pro677A, Ser318A and hydrophobic interactions with Thr319A, Phe321A, Thr462A, Asn628A and Val675A amino acids of protein chain (Fig.2C). (binding affinity  $-9.0 \text{ kcal/mol}$ )

Compound 2c binds with the protein chain by pi-cation interaction (Arg349A), pi-alkyl interactions (Val315A, Pro323A, Pro461A and Pro677A) and hydrophobic interaction (Thr319A, Phe321A, Phe326A, Glu350A, Thr394A, Cys395A, Phe396A, Tyr456A, Arg457A, Asn459A, Thr462A, Asn628A and Met629A) (Fig.2D). (binding affinity  $-8.8 \text{ kcal/mol}$ ).

Compound 2d forms hydrogen bonds (Asn628A), pi-alkyl (Pro323A, Pro461A and Pro677A) and hydrophobic interactions (Val315A, Thr319A, Phe321A, Phe326A, Glu350A, Thr394A, Cys395A, Phe396A, Tyr456A, Arg457A, Asn459A, Thr462A, Pro323A) with the protein. (Fig.2E). (binding affinity  $-8.7 \text{ kcal/mol}$ )

Compound 2e binds with Tyr32A, Aal130A, Lys780A (pi-alkyl interactions), Lys47A (pi-cation interaction), Tyr129A, His133A,





Asp135A, Asn138A, Cys139A, Thr141A, Ser709A, Thr710A, Asp711A, Asn781A and Ser784A (hydrophobic interaction) amino acids of RdRp protein chain (Fig.2F). (binding affinity -8.0 kcal/mol)

Similarly, binding site analysis for compound 3a demonstrate that it forms one hydrogen bond with Tyr346A, six pi-alkyl interactions with Pro328A, Val330A, Ala379A, Ala382A, Phe396A and Val398A. Ten hydrophobic interactions with Pro323A, Thr324A, Gly327A, Arg349A, Pro378A, Ala383A, Ser397A, Ala399A, Ser664A. One pi-sigma, one pi-sulfer and one amide-pi-stacking interactions with Val675A, Met666A and Phe326A respectively. (Fig.2G). (binding affinity -9.2 kcal/mol)

Compound 3b interacts through pi-pi staking (Tyr129A), pi-alkyl interaction (Tyr32A, Ala130A, and Lys780A), and hydrogen bonding (Lys47A) and hydrophobic interaction (His133A, Phe134A, Asp135A, Asn138A, Cys139A, Asp140A, Thr141A, Leu142A, Ser709A, Asn781A and Ser784A) with targeted protein chain. (Fig.2H). (binding affinity -8.7 kcal/mol)

Compound 3c interacts with NSP12 chain of RdRp by pi-alkyl interactions (Val315A, Pro323A, Cys395A, Pro461A, Pro677A), pi-cation interaction (Arg349A) and hydrophobic interactions (Ser318A, Thr319A, Phe321A, Glu350A, Thr394A, Phe396A, Tyr456A, Arg457A, Asn459A, Leu460A, Thr462A, Asn628A) (Fig.2I). (binding affinity -8.4 kcal/mol)

Compound 3d its binds with protein chain by pi-alkyl interactions (Ala130A, Lys780A), pi-cation interaction (Lys47A), and hydrophobic interactions (Tyr32A, Ala46A, Tyr129A, His133A, Asp135A, Asn138A, Cys139A, Thr141A, Ser709A, Thr710A, Asn781A and Ser784A) (Fig.2J). (binding affinity -8.4 kcal/mol)

Compound 3e inhibits the function of RdRp protein by binding with the given amino acids: Cys139A and Lys780A (pi-alkyl interactions), Lys47A (pi-cation interaction), and Tyr32A, Ala46A, Tyr129A, His133A, Asp135A, Asn138A, Asp140A, Thr141A, Ser709A, Thr710A, Asp711A, Asn781A and Ser784A (hydrophobic interactions) (Fig.2K). (binding affinity -8.3 kcal/mol)

Compound 4a forms three pi-alkyl interactions (Tyr32A, Ala130A and Lys780A), one pi-alkyl interaction with Lys47A and nine hydrophobic interactions with Tyr129A, His133A, Asn138A, Cys139A, Thr141A, Ala706A, Ser709A, Asn781A and Ser784A amino acids. (Fig.2L). (binding affinity -8.4 kcal/mol)

Compound 4b forms six pi-alkyl interactions with Pro328A, Leu329A, Arg331A, Ala382A, Phe396A and Val398A, one pi-pi stacking with Tyr273A and two hydrophobic interactions with Leu270A and Val330A to stop the action of enzymic protein (Fig.2M). (binding affinity -8.2 kcal/mol)

Compound 4c interacts with protein chain by six pi-alkyl interactions (Pro328A, Leu329A, Val330A, Ala382A, Phe396A and Val398A) and eleven hydrophobic interactions (Leu270A, Leu271A, Tyr273A, Thr324A, Ser325A, Phe326A, Pro378A, Ala379A, Leu387A, Ser397A and Met666A) (Fig.2N). (binding affinity -8.1 kcal/mol)

Compound 4d its forms two pi-alkyl interactions with Tyr32A, Ala130A, two hydrogen bonding interactions with His133A and Ser709A and ten hydrophobic interactions with Lys47A, Tyr129A, Asn138A, Cys139A, Thr141A, Leu142A, Ala706A, Thr710A, Asn781A and Ser784A of protein chain (Fig.2O). (-8.0 kcal/mol)

Compound 5a forms three pi-alkyl interactions with Leu371A, Leu372A and Ala375A, three hydrophobic interactions with Phe506A, Leu514A and Tyr515A, one pi-sulphur and one pi-sigma interactions with Phe368A and Trp509A respectively of NSP12 chain of RdRp of SARS-CoV-2 (Fig.2P). (binding affinity -9.0 kcal/mol)

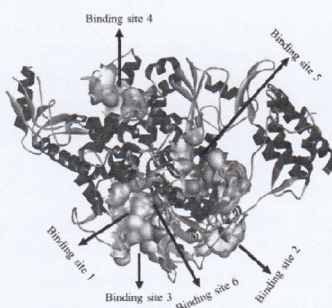
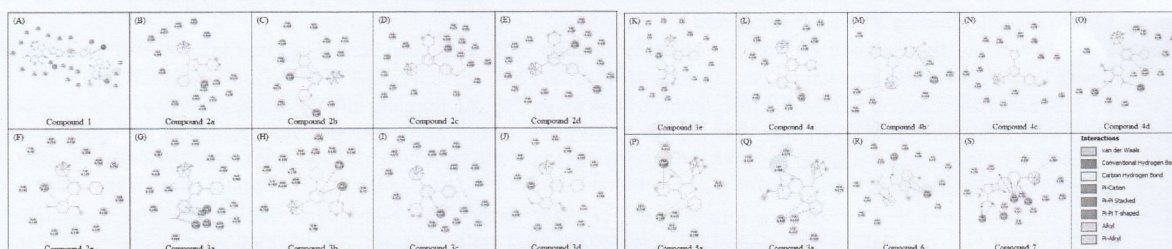
Compound 5b binds with Leu371A, Leu372A and Ala375A amino acids through pi-alkyl interaction, Phe368A with pi-sulphur interaction and Phe506A, Trp509A, Leu514A, Tyr515A by hydrophobic interactions. In this way it inhibits the action of protein (Fig.2Q). (binding affinity -8.6 kcal/mol)

Compound 6 binds with Leu371A (hydrogen bond), Phe340A, Leu372A, Ala375A and Tyr515A (pi-alkyl interactions), Trp509A (pi-pi stacking), Phe368A, Tyr374A, Met380A, His381A, Pro505A, Phe506A, Leu514A and Ser518A (hydrophobic interaction) amino acids with -8.9 kcal/mol binding energy with interacting protein chain (Fig.2R) (binding affinity -8.9 kcal/mol).

Compound 7 binds with Tyr32A, His133A, Lys714A, Ser709A (hydrogen bonding), Lys780A (pi-alkyl interaction) and Ala46A, Lys47A, Tyr129A, Asp135A, Asn138A, Ala706A, Thr710A, Asp711A, Gln773A, Gly774A, Asn781A and Ser784A (hydrophobic interactions) amino acids of ligand protein (Fig.2S) (binding affinity -8.2 kcal/mol).

The details analysis of protein-Ligand interactions with various ferrocenyl compounds with NSP12 chain of RdRp of SARS Co-V-2 shows compounds 2a, 2b, 2c, 2d and 3c surrounded by val315A, Thr319A, Phe321A, Pro323A, Arg349A, Glu350A, Thr394A, Cys395A, Phe396A, Pro461A, Asn628A and Pro677A (binding site -1). Compounds 5a, 5b and 6 interact with binding site 2 which contain Phe368A, Leu371A, Leu372A, Ala375A, Phe506A, Trp509A, Leu514A and Tyr515A amino acids. Compounds 4b and 4c binds with binding site 3 containing amino acids Leu270A, Tyr273A, pro328A, Leu 329A, Val 330A, Phe 396A and Val 398A. Compounds 2e, 3b, 3d, 3e, 4a, 4d and 7 interact with binding site 4 having amino acid Tyr32A, Lys47A, Tyr129A, His133A, Asn138A, Ser709A, Asn781A and Ser784A. Compound 1 and 3a binds with protein chain with two completely different binding site namely binding site 5 (Asn497A, Lys621A, Asp623A, Tyr455A, Lys500A, Arg553A, Val557A, Pro620A, Ala685A, Asn496A, Ser501A, Lys545A, Lys551A, Arg555A, Ala558A, Gly559A, Arg569A, Asp618A, Tyr619A, Ser682A, Gly683A, Cys622A) and 6 (Tyr346A, Pro328A, Val330A, Ala379A, Ala382A, Phe396A, Val398A, Pro323A, Thr324A, Gly327A, Arg349A, Pro378A, Ala383A, Ser397A, Ala399A, Ser664A, Val675A, Met666A, Phe326A. (Fig.1).



**Fig 1:** Binding sites of with NSP12 chain of RdRp of SARS Co-V-2**Fig 2:** 2D representation of 19 compounds against RNA-dependent RNA polymerase of SARS-CoV-2**Absorption, distribution, Metabolism and Excretion (ADME) of A, G and D**

ADME characteristics are very important measuring tool for drug developing process [48]. Large number of the drugs candidates fails due to poor effectiveness like low bioavailability, inadequate intestinal absorption and poor metabolic stability [Prueksaritanont et al. 2012; Daina et al. 2017; Daina et al. 2016; Dania et al. 2017]. The parameter ( $\log P_{OW}$ ) represents the Lipophilicity [Ozkan et al. 2020] and  $\log S$  denotes water solubility. The said parameters should be less than or equal to 5 and less than 6 respectively. The Lipinski's rule says the drug which is consumed orally should have hydrogen bond donor site less than or equal to five, hydrogen bond acceptor less than or equal to ten, molecular mass less than 500 gm/mol and  $\log P$  values less than 5 [Ghose et al. 1999; Egan et al. 2000; Lipinski 2004]. The gastrointestinal (GI) absorption and BBB (blood-brain barrier) should be high and No respectively for an effective drug. [Terasaki 2017].

In this computational investigation all biological properties of 19 ferrocene derivatives were summarized in Table 2, Table 3, Table 4 and Table 5. The results from this study revealed that out of the 19 compounds Two compounds 3d and 3e obeyed Lipinski's rule without any violation, they are moderately soluble in water, having molecular weight less than 500 g/mol, less than 5 H-bond donor site and less than 10 H-bond acceptor site, high GI absorption value and the compounds not able to cross BBB (blood-brain barrier). So compounds may be a good choice as drug. Although the binding affinity of compound 1 is highest than the other 18 compounds, but the ADME analysis showed it violates the Lipinski rule as well as it is insoluble in water.

**DFT study**

Compounds Optimize geometry	HOMO	LUMO	$E_{HOMO-LUMO}$	Single point energy kJ/mol
3d	 -5.246eV	 -1.075eV	-4.165	-6885948.581
3e	 -5.196eV	 -1.127eV	-4.063	-7186146.611

Using the DFT calculations, the structures of ferrocene-based compounds are optimized, zero-point energy and HOMO, LUMO have





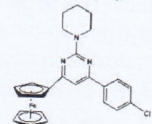
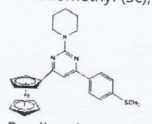
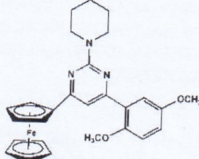
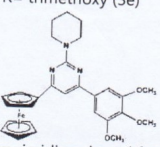
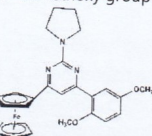
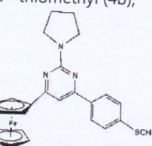
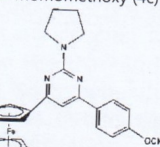
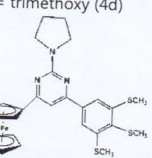
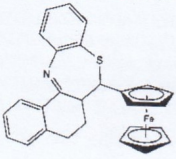
been calculated. Energy gap between HOMO and LUMO is a useful to understand the reactivity of compounds. The large  $E_{\text{HOMO}}-E_{\text{LUMO}}$  energy gap indicates the molecule is hard and easily participate in reaction whereas small  $E_{\text{HOMO}}-E_{\text{LUMO}}$  energy gap determines the molecule is soft and easily participate in the reaction. In the main manuscript, The above data from DFT calculation have been summarized in Table 6 for two compounds which shows promising binding affinity as well as physiochemical and pharmacokinetic properties. The data of other compounds are summarized in Supporting manuscript.

**Table 1-** The summarized docking score.

Name	Binding Energy [kcal/mol]	Hydrogen bonds	Other interactions
1,1'-diarylated ferrocene derivative (1)  Pyrimidine based ferrocene derivative linked with the morpholine group and substituted phenyl group	-9.6	ASN(497A),LYS(621A)	TYR(455A),ASN(496A),LYS(500A),SER(501A),LYS(545A),LYS(551A),ARG(553A),ARG(555A),VAL(557A),ALA(558A),GLY(559A),ARG(569A),ASP(618A),TYR(619A),PRO(620A),CYS(622A),ASP(623A),SER(682A),GLY(683A),ALA(685A),LYS(798A)
R=H (2a) 	-8.8		VAL(315A),SER(318A),THR(319A),PHE(321A),PRO(323A),PHE(326A),ARG(349A),GLU(350A),THR(394A),CYS(395A),PHE(396A),ARG(457A),ASN(459A),PRO(461A),ASN(628A),PRO(677A)
R= dimethyl group (2b) 	-9.0	PHE(396A)	VAL(315A),SER(318A),THR(319A),PHE(321A),PRO(323A),ARG(349A),CYS(395A),PRO(461A),THR(462A),ASN(628A),VAL(675A),PRO(677A)
R= mono methoxy group (2c), 	-8.8		VAL(315A),THR(319A),PHE(321A),PRO(323A),PHE(326A),ARG(349A),GLU(350A),THR(394A),CYS(395A),PHE(396A),TYR(456A),ARG(457A),ASN(459A),PRO(461A),THR(462A),ASN(628A),PRO(677A)
R= hydroxyl group (2d), 	-8.7	ASN(628A)	VAL(315A),THR(319A),PHE(321A),PRO(323A),PHE(326A),ARG(349A),GLU(350A),THR(394A),CYS(395A),PHE(396A),TYR(456A),ARG(457A),ASN(459A),PRO(461A),THR(462A),PRO(677A)
R= dimethoxy group (2e) 	-8.0		TYR(32A),LYS(47A),TYR(129A),ALA(130A),HIS(133A),ASP(135A),ASN(138A),LYS(139A),THR(141A),SER(709A),THR(710A),ASP(711A),LYS(780A),ASN(781A),SER(784A)
pyrimidines based ferrocenyl compounds cojugateswith piperidine group R= methoxy group (3a) 	-9.2	TYR(346A),	PRO(323A),THR(324A),PHE(326A),GLY(327A),PRO(328A),VAL(330A),ARG(349A),PRO(378A),ALA(379A),ALA(382A),ALA(383A),LEU(387A),PHE(396A),SER(397A),VAL(398A),ALA(399A),SER(664A),MET(666A),VAL(675A)





R= chloro (3b), 	-8.7	LYS(47A)	TYR(32A),TYR(129A),ALA(130A),HIS(133A),PHE(134A),ASP(135A),ASN(138A),CYS(139A),ASP(140A),THR(141A),LEU(142A),SER(709A),LYS(780A),ASN(781A),SER(784A)
R= thiomethyl (3c), 	-8.4		VAL(315A),SER(318A),THR(319A),PHE(321A),PRO(323A),ARG(349A),GLN(350A),THR(394A),CYS(395A),PHE(396A),TYR(456A),ARG(457A),ASN(459A),LEU(460A),PRO(461A),THR(462A),ASN(628A),PRO(677A)
R= dimethoxy (3d) 	-8.4		TYR(32A),ALA(46A),LYS(47A),TYR(129A),ALA(130A),HIS(133A),ASP(135A),ASN(138A),LYS(139A),THR(141A),SER(709A),THR(710A),LYS(780A),ASN(781A),SER(784A)
R= trimethoxy (3e) 	-8.3		TYR(32A),ALA(46A),LYS(47A),TYR(129A),ALA(130A),HIS(133A),ASP(135A),ASN(138A),LYS(139A),ASP(140A),THR(141A),SER(709A),THR(710A),ASP(711A),LYS(780A),ASN(781A),SER(784A)
pyrimidines based ferrocenyl compounds conjugates with pyrrolidine group			
R= dimethoxy group (4a) 	-8.4		TYR(32A),LYS(47A),TYR(129A),ALA(130A),HIS(133A),ASN(138A),LYS(139A),THR(141A),ALA(706A),SER(709A),LYS(780A),ASN(781A),SER(784A)
R= thiomethyl (4b), 	-8.2		LEU(270A),TYR(273A),PRO(328A),LEU(329A),VAL(330A),ARG(331A),ALA(382A),PHE(396A),VAL(398A)
R= momomethoxy (4c) 	-8.1		LEU(270A),LEU(271A),TYR(273A),THR(324A),SER(325A),PHE(326A),PRO(328A),LEU(329A),VAL(330A),PRO(378A),ALA(379A),ALA(382A),LEU(387A),PHE(396A),SER(397A),VAL(398A),MET(666A)
R= trimethoxy (4d) 	-8.0	SER(709A)	TYR(32A),LYS(47A),TYR(129A),ALA(130A),HIS(133A),ASN(138A),LYS(139A),THR(141A),LEU(142A),ALA(706A),THR(710A),ASN(781A),SER(784A)
Thiazepin derivative (5a) 	-9.0		PHE(368A),LEU(371A),LEU(372A),ALA(375A),PHE(506A),TRP(509A),LEU(514A),TYR(515A)





Thiazepin derivative	OCH <sub>3</sub>	(5b)	-8.6	LEU(371A)	PHE(340A),PHE(368A),LEU(372A),TYR(374A),ALA(375A),MET(380A),HIS(381A),PRO(505A),PHE(506A),TRP(509A),LEU(514A),TYR(515A),SER(518A)
 Mefloquine derivative (6)			-8.9		PHE(368A),LEU(371A),LEU(372A),ALA(375A),PHE(506A),TRP(509A),LEU(514A),TYR(515A)
 Ferrocenyl 6-aminopenicillanic acid bioconjugate (7)			-8.2	TYR(32A), HIS(133A), SER(709A), LYS(714A),	ALA(46A),LYS(47A),TYR(129A),ASP(135A),ASN(138A),ALA(706A),THR(710A),ASP(711A),GLN(773A),GLY(774A),LYS(780A),ASN(781A),SER(784A)

## Conclusions

In summary, we have screened 45 biologically active ferrocenyl compounds against NSP12 chain of RdRp of SARS-CoV-2 and among 19 compounds shows greater potential in comparison to remdesivir. Antiviral hepatitis C ferrocenyl derivative, 1,1'-diarylated ferrocene derivative (1) shows highest binding affinity in comparison with all other ferrocenyl derivative and remdesivir. One of the anti-bacterial, (7) (staphylococcus aureus and staphylococcus epidermidis) shows a promising result and other 17 anti-parasitic ferrocenyl compounds (Entamoeba histolytica, Plasmodium falciparum) also can have potential to inhibit the function of RdRp. Although compound (1) shows highest binding affinity but according to ADME study it is not suitable for drug candidate. Compounds 3d and 3e show binding affinity -8.4 and -8.3 respectively, are good choice because they are moderately soluble in water, obeys Lipinski rule, high gastrointestinal absorption and not able to cross blood-brain barrier. This study is the first in-silico docking study of ferrocene-based compounds against RdRp protein of COVID-19 virus and we believe the outcomes will be useful in formulating ferrocene based organometallic compound to treat COVID-19 disease.

## References

- Aouidate, Adnane, et al. "Computer aided drug design based on 3D-QSAR and molecular docking studies of 5-(1H-indol-5-yl)-1, 3, 4-thiadiazol-2-amine derivatives as PIM2 inhibitors: a proposal to chemists." *In Silico Pharmacology* 6.1 (2018): 1-14.
- Alizadehmohajer, Negin, et al. "Screening of potential inhibitors of COVID-19 with repurposing approach via molecular docking." *Network Modeling Analysis in Health Informatics and Bioinformatics* 11.1 (2022): 1-11.
- Biot, Christophe, et al. "Synthesis and antifungal activity of a ferrocene-fluconazole analogue." *Bioorganic & medicinal chemistry letters* 10.8 (2000): 839-841.
- Biot, Christophe, et al. "L'activité antipaludique de la ferroquine: de la recherche à la clinique." (2011).
- Channotiya, Jiya, et al. "In-silico and Molecular Docking Studies on Germacrene A Synthase enzyme and sesquiterpene lactone (Lactucin) involved in antimalarial activity of Cichorium intybus." *Network Modeling Analysis in Health Informatics and Bioinformatics* 10.1 (2021): 1-10.
- DeLano, Warren L. "Pymol: An open-source molecular graphics tool." *CCP4 News. Protein Crystallogr* 40.1 (2002): 82-92.
- Daina, Antoine, and Vincent Zoete. "A boiled-egg to predict gastrointestinal absorption and brain penetration of small molecules." *ChemMedChem* 11.11 (2016): 1117-1121.
- Daina, Antoine, Olivier Michielin, and Vincent Zoete. "iLOGP: a simple, robust, and efficient description of n-octanol/water partition coefficient for drug design using the GB/SA approach." *Journal of chemical information and modeling* 54.12 (2014): 3284-3301.
- Wang, Chih-Feng, et al. "Nanoindentation-enhanced tip-enhanced Raman spectroscopy." *The Journal of Chemical Physics* 154.24 (2021): 241101.
- Gadhachanda, Venkat R., et al. "Ferrocene-based inhibitors of hepatitis C virus replication that target NS5A with low picomolar in vitro antiviral activity." *Bioorganic & Medicinal Chemistry Letters* 28.21 (2018): 3463-3471.
- Deb, Subrata, et al. "ADME and pharmacokinetic properties of remdesivir: its drug interaction potential." *Pharmaceuticals* 14.7 (2021): 655.
- Kealy, T. J., and P. L. Pauson. "A new type of organo-iron compound." *Nature* 168.4285 (1951): 1039-1040.
- Wang, Xueqing, and Yuanfang Guan. "COVID-19 drug repurposing: a review of computational screening methods, clinical trials, and protein interaction assays." *Medicinal research reviews* 41.1 (2021): 5-28.





- Khaerunnisa, Siti, et al. "Potential inhibitor of COVID-19 main protease (Mpro) from several medicinal plant compounds by molecular docking study." *Preprints* 2020 (2020): 2020030226.
- Shah, Sapan, et al. "Exploring the active constituents of *Oroxylum indicum* in intervention of novel coronavirus (COVID-19) based on molecular docking method." *Network Modeling Analysis in Health Informatics and Bioinformatics* 10.1 (2021): 1-12.
- Shang, J., et al. "Structure of 2019-nCoV chimeric receptor-binding domain complexed with its receptor human ACE2." *Worldw. Protein Data Bank* (2020).
- Pang, Yanqing, et al. "Design, synthesis, and biological evaluation of novel selenium-containing iso combretastatins and phenstatins as antitumor agents." *Journal of Medicinal Chemistry* 60.17 (2017): 7300-7314.
- Chohan, Zahid H. "Antibacterial and antifungal ferrocene incorporated dithiothione and dithioketone compounds." *Applied organometallic chemistry* 20.2 (2006): 112-116.
- García, Jessica J. Sánchez, et al. "Polycyclic ferrocenyl (dihydro) thiazepine derivatives: Diastereo-selective synthesis, characterization, electrochemical behavior, theoretical and biological investigation." *Journal of Inorganic Biochemistry* 166 (2017): 141-149.
- Jayaweera, M., et al. "Transmission of COVID-19 virus by droplets and aerosols." *A critical review on the unresolved dichotomy* 2020: 188.
- Khaerunnisa, Siti, et al. "Potential inhibitor of COVID-19 main protease (Mpro) from several medicinal plant compounds by molecular docking study." *Preprints* 2020 (2020): 2020030226.
- Lal, Bhajan, et al. "Miscellaneous applications of ferrocene-based peptides/amides." *Applied Organometallic Chemistry* 25.12 (2011): 843-855.
- Lipinski, C. A., et al. "In vitro models for selection of development candidates: experimental and computational approaches to estimate solubility and permeability in drug discovery and development settings." *Adv Drug Deliv Rev* 23.1 (1997): 3-25.
- Vickers, Neil J. "Animal communication: when i'm calling you, will you answer too?." *Current biology* 27.14 (2017): R713-R715.
- Ludwig, Beatrice S., João DG Correia, and Fritz E. Kühn. "Ferrocene derivatives as anti-infective agents." *Coordination Chemistry Reviews* 396 (2019): 22-48.
- Khaerunnisa, Siti, et al. "Potential inhibitor of COVID-19 main protease (Mpro) from several medicinal plant compounds by molecular docking study." *Preprints* 2020 (2020): 2020030226.
- Lal, Bhajan, et al. "Miscellaneous applications of ferrocene-based peptides/amides." *Applied Organometallic Chemistry* 25.12 (2011): 843-855.
- Lewandowski, Eric M., et al. "Antibacterial properties and atomic resolution X-ray complex crystal structure of a ruthenocene conjugated  $\beta$ -lactam antibiotic." *Chemical Communications* 51.28 (2015): 6186-6189.
- Özkan, Hamdi, and Şevki Adem. "Synthesis, Spectroscopic Characterizations of Novel Norcantharimides, Their ADME Properties and Docking Studies Against COVID-19 Mpr." *ChemistrySelect* 5.18 (2020): 5422-5428.
- Peter, Sijongesonke, and Blessing AtimAderibigbe. "Ferrocene-based compounds with antimalaria/anticancer activity." *Molecules* 24.19 (2019): 3604.
- Parveen, Humaira, et al. "Synthesis, characterization and biological evaluation of novel 6-ferrocenyl-4-aryl-2-substituted pyrimidine derivatives." *European journal of medicinal chemistry* 45.8 (2010): 3497-3503.
- Ruiz, Isaac, Stéphane Chevaliez, and Jean-Michel Pawlotsky. "Next-generation direct-acting antiviral drug-based regimens for hepatitis C." *Current Hepatology Reports* 16.3 (2017): 184-191.
- Prueksaritanont, Thomayant, and Cuyue Tang. "ADME of biologics—what have we learned from small molecules?." *The AAPS journal* 14.3 (2012): 410-419.
- Shoukat, Hamza, Ataf Ali Altaf, and Amin Badshah. "Ferrocene-Based Metallodrugs." *Advances in Metallodrugs: Preparation and Applications in Medicinal Chemistry* (2020): 115-136.
- Yin, Wanchao, et al. "Structural basis for inhibition of the RNA-dependent RNA polymerase from SARS-CoV-2 by remdesivir." *Science* 368.6498 (2020): 1499-1504.